H2AX phosphorylation marks gemcitabine-induced stalled replication forks and their collapse upon S-phase checkpoint abrogation

Brett Ewald, Deepa Sampath, and William Plunkett

Department of Experimental Therapeutics, The University of Texas M. D. Anderson Cancer Center, Houston, Texas and The University of Texas Graduate School of Biomedical Sciences, Houston, Texas

Abstract

Gemcitabine is a nucleoside analogue that is incorporated into replicating DNA, resulting in partial chain termination and stalling of replication forks. The histone variant H2AX is phosphorylated on Ser^{139} (γ-H2AX) and forms nuclear foci at sites of DNA damage. Here, we characterize the concentration- and time-dependent phosphorylation of H2AX in response to gemcitabine-induced stalled replication forks. The number of γ-H2AX foci increased with time up to 2 to 6 h after exposure to gemcitabine, whereas longer exposures did not cause greater phosphorylation or increase cell death. The percentage of γ-H2AX–positive cells increased with concentrations of gemcitabine up to 0.1 μmol/L, and γ-H2AX was most evident in the S-phase fraction. Phosphorylation of ataxia-telangiectasia mutated (ATM) on Ser^{1981} was also associated with S-phase cells and colocalized in the nucleus with phosphorylated H2AX foci after gemcitabine exposure. Chemical inhibition of ATM, ATM- and Rad3-related, and DNA-dependent protein kinase blocked H2AX phosphorylation. H2AX and ATM phosphorylation were associated with inhibition of DNA synthesis, S-phase accumulation, and activation of the S-phase checkpoint pathway (Chk1/Cdc25A/cyclin-dependent kinase 2). Exposure of previously gemcitabine-treated cultures to the Chk1 inhibitor 7-hydroxystaurosporine (UCN-01) caused a 10-fold increase in H2AX phosphorylation, which was displayed as an even pan-nuclear staining. This increased phosphorylation was not due to apoptosis-induced DNA fragmentation and was associated with the S-phase fraction and decreased reproductive viability. Thus, H2AX becomes phosphorylated and forms nuclear foci in response to gemcitabine-induced stalled replication forks, and this is greatly increased upon checkpoint abrogation. [Mol Cancer Ther 2007;6(4):1239–48]

Introduction

Nucleoside analogues are antimetabolites effective in the treatment of a wide variety of solid tumors and hematologic malignancies (1). On cellular entry, these nucleic acid antagonists are phosphorylated to a triphosphate form and incorporated into DNA (2, 3). Incorporation causes steric hindrance of extending replication forks, leading to fork stalling, which induces S-phase checkpoint activation, a subsequent decrease in initiation of replication origins (4), and S-phase arrest (5, 6). These events are likely necessary for replication fork stabilization and prevention of irreversible fork collapse (7). Nucleoside analogue incorporation into DNA is critical for toxicity, and thus this class of agents shows specificity for S-phase cells (2, 3, 8).

The checkpoint kinase Chk1 is an important regulator of the cell cycle machinery. On recognition of replication stress by sensor molecules, Chk1 kinase is activated by phosphorylation on Ser^{317} and Ser^{345} and plays a key role in relaying signals to effectors (9). In the presence of stalled replication forks, Chk1 inhibits Cdc25A phosphatase from dephosphorylating the Tyr^{15} residue of cyclin-dependent kinase 2 (Cdk2; ref. 10). Thus, in response to replication stress, the inactive Tyr^{15}-phosphorylated form of Cdk2 is unable to initiate replication origins (11), inducing cell cycle arrest. Direct pharmacologic inhibition, interference with Chk1 protein maturation, or siRNA knockdown of Chk1 induces checkpoint abrogation of cells blocked in S-G_2 phase, resulting in greater than additive cell killing (6, 12–14). The Chk1 kinase inhibitor 7-hydroxystaurosporine (UCN-01), which effectively abrogates the S and G_2 checkpoints, is currently being investigated in phase I and II trials either alone or in combination with cytotoxic agents (15–17).

The molecular mechanisms that sense aberrant DNA structures at stalled replication forks and initiate cellular responses are not well defined. Ataxia-telangiectasia mutated (ATM) has been identified as a sensor that is a key signaling molecule for initiating cell cycle arrest, DNA repair, and apoptosis (18). Following DNA damage, nuclear ATM dimers disassociate into active monomers on autophosphorylation of Ser^{1981} and localize to sites of DNA damage (19). As a central kinase in triggering cellular responses, ATM can phosphorylate several substrates

Received 10/12/06; revised 1/26/07; accepted 2/21/07.

Grant support: Grants CA32839 and CA55164 and Cancer Center support grant CA16672 from the National Cancer Institute Department of Health and Human Services.

The costs of publication of this article were defrayed in part by the payment of page charges. This article must therefore be hereby marked *advertisement* in accordance with 18 U.S.C. Section 1734 solely to indicate this fact.

Requests for reprints: William Plunkett, Department of Experimental Therapeutics, Unit 71, The University of Texas M. D. Anderson Cancer Center, 1515 Holcombe Boulevard, Houston, TX 77030.
Phone: 713-792-3335; Fax: 713-794-4316.
E-mail: wplunket@mdanderson.org

doi:10.1158/1535-7163.MCT-06-0633

involved in the cell cycle checkpoints, including Chk1, Chk2, and p53. ATM has also been shown to colocalize at sites of ionizing radiation–induced DNA damage (20) and to phosphorylate the histone variant H2AX on Ser^{139} (21). Along with ATM, two other ATM-related kinases, ATM- and Rad3-related (ATR) and DNA-dependent protein kinase, may also be capable of phosphorylating H2AX (22).

Phosphorylated H2AX (γ-H2AX) is a well-known marker of DNA damage that forms nuclear foci containing thousands of molecules at DNA damage sites (23, 24). The function of γ-H2AX has not been elucidated; however, evidence suggests that these molecules may recruit checkpoint proteins to sites of DNA damage and play a role in DNA repair (25). Depending on the nature of the DNA lesion, colocalization of γ-H2AX can occur with other molecules, including 53BP1, Mre11, Rad50, and Nbs1, thus further suggesting its involvement in DNA repair (20, 25). Recently, phosphorylation of H2AX has been shown to be required for the repair of double-strand breaks using sister chromatid recombination (26) and for DNA fragmentation during apoptosis (27, 28). Dephosphorylation of H2AX by protein phosphatase 2A may be associated with efficient DNA repair (29). $H2AX^{-/-}$ mice display increases in chromosomal rearrangements and accelerated tumor formation in the absence of p53, suggesting a role for H2AX in genomic stability (30–32). Although originally thought of as a molecular sensor for double-strand breaks, the involvement of γ-H2AX in recognizing other types of DNA damage and cellular stresses is becoming more evident (22, 33–35). Whether H2AX is phosphorylated and forms nuclear foci at sites of nucleoside analogue–induced stalled replication forks has not been studied in detail (36).

Although the mechanisms by which this drug class induces cell killing have been well studied, the molecules that sense nucleoside analogue–induced stalled replication forks are unknown. Proficient molecular recognition of nucleoside analogue incorporation may lead to DNA repair and drug resistance, which could form the basis of less than optimal clinical response. Therefore, we investigated the molecular mechanisms by which cells sense nucleoside analogue incorporation into DNA using gemcitabine as a model drug. This study identifies H2AX phosphorylation as a pharmacodynamic indicator of gemcitabine-induced stalled replication forks that correlates with cellular reproductive viability.

Materials and Methods

Cell Culture

ML-1 and OCI-AML3, human adult myelogenous leukemia cell lines, were gifts from Dr. Michael B. Kastan (St. Jude Children's Research Hospital, Memphis, TN) and Dr. Michael Andreeff (The University of Texas M. D. Anderson Cancer Center, Houston, TX), respectively. Both cell lines were maintained in exponential growth phase in RPMI 1640 supplemented with 10% heat-inactivated fetal bovine serum (Invitrogen, Carlsbad, CA) at 37°C (5% CO_2) in a humidified atmosphere. Population doubling times were ~18 to 22 h.

Chemicals and Antibodies

The nucleoside analogues gemcitabine and troxacitabine were kindly provided by Dr. L.W. Hertel (Lilly Research Laboratories, Indianapolis, IN) and Dr. Henriette Gourdeau (Biochem Pharma, Montreal, Canada), respectively. The cytarabine used in the investigations was purchased from Sigma-Aldrich (St. Louis, MO). UCN-01 (NSC 638850) was provided by the Drug Synthesis and Chemistry Branch, Division of Cancer Treatment, National Cancer Institute (Bethesda, MD). Aliquots of UCN-01 were stored at a concentration of 10 mmol/L in DMSO at −20°C and diluted in serum-free medium immediately before each experiment. Z-VAD was purchased from MP Biomedicals (Solon, OH). All other chemicals were of reagent grade.

Mouse monoclonal antibodies to Cdk2, phospho-H2AX (Ser^{139}), phospho-ATM (Ser^{1981}), and rabbit polyclonal antibodies to Chk2 and phospho-H2AX (Ser^{139}) were purchased from Upstate Biotechnology (Charlottesville, VA). Rabbit polyclonal antibodies to phospho-Chk1 (Ser^{317}), phospho-Chk2 (Thr^{68}), and phospho-Cdk2 (Tyr^{15}) and rabbit monoclonal antibody to phospho-Chk1 (Ser^{345}) were purchased from Cell Signaling Technology (Beverly, MA). Mouse monoclonal antibody to Chk1 was purchased from Santa Cruz Biotechnology (Santa Cruz, CA). Mouse anti–poly(ADP-ribose) polymerase was purchased from BD PharMingen International (San Diego, CA). Mouse monoclonal antibody to β-actin was purchased from Sigma-Aldrich. Alexa Fluor 488, Alexa Fluor 594, and Alexa Fluor 680 fluorescent secondary antibodies were purchased from Molecular Probes (Eugene, OR). IRDye 800 goat anti-rabbit immunoglobulin G antibody was purchased from Rockland Immunochemicals (Gilbertsville, PA). FITC-conjugated goat anti-mouse immunoglobulin G antibody was purchased from Jackson ImmunoResearch Laboratories, Inc. (West Grove, PA).

Immunoblotting Analysis

Cell lysates were diluted with 4× SDS sample loading buffer containing 200 mmol/L Tris-Cl (pH 6.8), 40% glycerol, 8% SDS, 0.1% bromphenol blue, and 10% β-mercaptoethanol. Lysates were then heated at 100°C for 5 min. Aliquots of total cell protein (75 μg) were loaded onto 10% SDS-polyacrylamide gels. Proteins were electrophoresed at a constant voltage (70–100 V) and transferred to nitrocellulose membranes (GE Osmonics Labstore, Minnetonka, MN) for 3 h at 300 mA. Membranes were blocked for 1 h with blocking buffer (Li-Cor Biosciences, Lincoln, NE) and then incubated overnight at 4°C with primary antibodies as indicated in the figure legends. Membranes were then incubated with fluorescent-conjugated secondary antibodies (1:5,000 dilution) for 1 h. The blots were visualized using an Odyssey Infrared Imaging System (Li-Cor Biosciences) according to the manufacturer's instructions.

Cell Cycle Analysis

Cells were washed with ice-cold PBS and fixed in 70% ethanol overnight at 4°C. Fixed cells were washed with PBS before incubation in 15 μg/mL propidium iodide

(Sigma-Aldrich) and 2.5 μg/mL RNase A (Roche, Indianapolis, IN) for 30 min. At least 10,000 cells were evaluated for fluorescence using a Becton Dickinson FACSCalibur flow cytometer (San Jose, CA).

Confocal Microscopy

Drug-treated or ionizing radiation–exposed (3.17 Gy/min) cultures were centrifuged onto slides, fixed in 4% paraformaldehyde, and permeabilized with 0.5% Triton X-100. After blocking with PBS containing 5% goat serum (Jackson ImmunoResearch Laboratories), cells were incubated with a primary antibody at a 500-fold dilution in 3% goat serum in PBS for 2 h followed by three washes with PBS containing 0.1% NP-40. Cells were incubated for 1 h with fluorescent-conjugated secondary antibodies (1:100 dilution), followed by three washes with PBS. Cell nuclei were stained and slides were mounted with ProLong Gold antifade reagent with 4′,6-diamidino-2-phenylindole (Molecular Probes). Coverslips were sealed with nail polish. Fluorescence was viewed with an Olympus Fluoview FV500 confocal microscope system (Olympus, Center Valley, PA) using a 60× objective. The projections of single slices were saved as TIF files.

Cytometric Analysis

Cells were harvested at indicated times after ionizing radiation (3.17 Gy/min) or drug treatment, washed twice with ice-cold PBS, fixed in 4% paraformaldehyde for 10 min at room temperature, and postfixed with 70% ethanol overnight at 4°C. The cells were washed in PBS and resuspended in 5% goat serum/PBS (Jackson ImmunoResearch Laboratories) for 1 h at room temperature to suppress nonspecific antibody binding. After centrifugation, the pellet was suspended in 100 μL of 3% goat serum containing the primary antibody (1:500 dilution) and incubated for 2 h at room temperature. The cells were centrifuged and resuspended in 250 μL of 3% goat serum containing a fluorescent-conjugated secondary antibody (1:100 dilution) for 1 h in the dark. The pellet was then washed twice and counterstained with propidium iodide (15 μg/mL; Sigma-Aldrich) containing 2.5 μg/mL RNase A (Roche) for 30 min at 4°C. Fluorescence of at least 10,000 cells was determined on a Becton Dickinson FACSCalibur flow cytometer.

DNA Synthesis Assay

Exponentially growing cells were exposed to gemcitabine for indicated times and incubated at 37°C. [^{3}H]Thymidine at 5 μCi/mL (60.9 Ci/mmol; Moravek Biochemicals, Brea, CA) was added 30 min before the end of incubation. Cells were harvested and diluted in 10-mL ice-cold PBS. Labeled cells were collected on glass fiber filters (Schleicher & Scheull, Riviera Beach, FL) using a Millipore vacuum manifold (Billerica, MA). The filters were washed with 5 drops of 1% sodium phosphate to prevent nonspecific binding before collection. Each sample was poured onto filters and gradually pulled through using a vacuum. Filters were washed twice with 5-mL ice-cold 0.4 N perchloric acid, rinsed with 70% ethanol and 100% ethanol, and allowed to dry in manifold. Radioactivity retained on the filter was determined by a liquid scintillation counter (Packard, Ramsey, MN).

Colony Formation Assay

Exponentially growing cultures were exposed to drugs for indicated times before being washed with PBS (37°C) and placed in fresh medium. Five hundred cells were distributed in MethoCult H4230 methylcellulose medium (Stem Cell Technologies, Vancouver, Canada) with added 1× Iscove's modified Dulbecco's medium (Invitrogen), $NaHCO_3$, and 5% L-glutamine, and then placed at 37°C in a six-well plate for 10 days. Colonies of ≥50 cells were counted under a dissecting microscope.

Results

H2AX Phosphorylation at Sites of Gemcitabine-Induced Stalled Replication Forks

To determine if there is an association between stalled replication forks, the S-phase population, and H2AX phosphorylation, the action of gemcitabine on the rate of DNA synthesis was investigated. Exposure of ML-1 cultures to gemcitabine caused inhibition of DNA synthesis by 90% within 1 to 2 h in a concentration-dependent fashion, as measured by a decrease in [^{3}H]thymidine incorporation (Fig. 1A). The decrease in DNA replication was associated with an accumulation of cells in S phase within 24 h (Fig. 1B). Next, we investigated the immunofluorescent detection of γ-H2AX to determine if the gemcitabine-induced stalled replication forks responsible for activation of the S-phase checkpoint also initiated γ-H2AX foci formation at sites of DNA incorporation. Distinct phosphorylated H2AX foci were evident in the nucleus of ML-1 cells by confocal microscopy within 2 h of exposure to 10 nmol/L gemcitabine and were similar to foci caused by ionizing radiation (Fig. 2A, *top*). Treatment with 100 nmol/L gemcitabine (2 h) caused an increased number of γ-H2AX foci per cell, but further increases in foci formation were not observed when cultures were exposed to 20 μmol/L drug (Fig. 2A, *top*). Nuclear foci were also evident in another acute myelogenous leukemia cell line, OCI-AML3, after exposure to

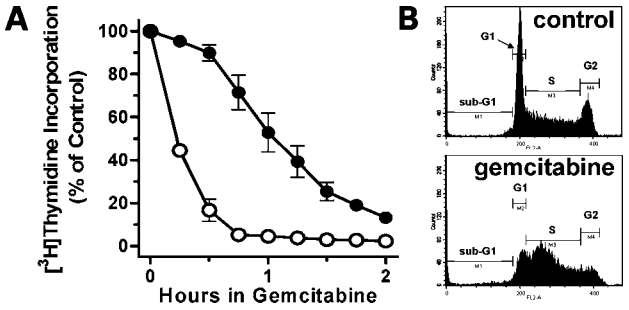

Figure 1. Decreased DNA synthesis and increased S-phase arrest caused by gemcitabine. **A,** effect of 10 nmol/L (●) or 100 nmol/L (○) gemcitabine on DNA synthesis, as measured by [^{3}H]thymidine incorporation. *Points,* mean of three independent experiments done in duplicate (n = 6); *bars,* SE. **B,** accumulation of cells in S phase after exposure to 10 nmol/L gemcitabine for 24 h, as measured by DNA content (propidium iodide). Cell populations representing sub-G_1, G_1, S, and G_2 phases are indicated.

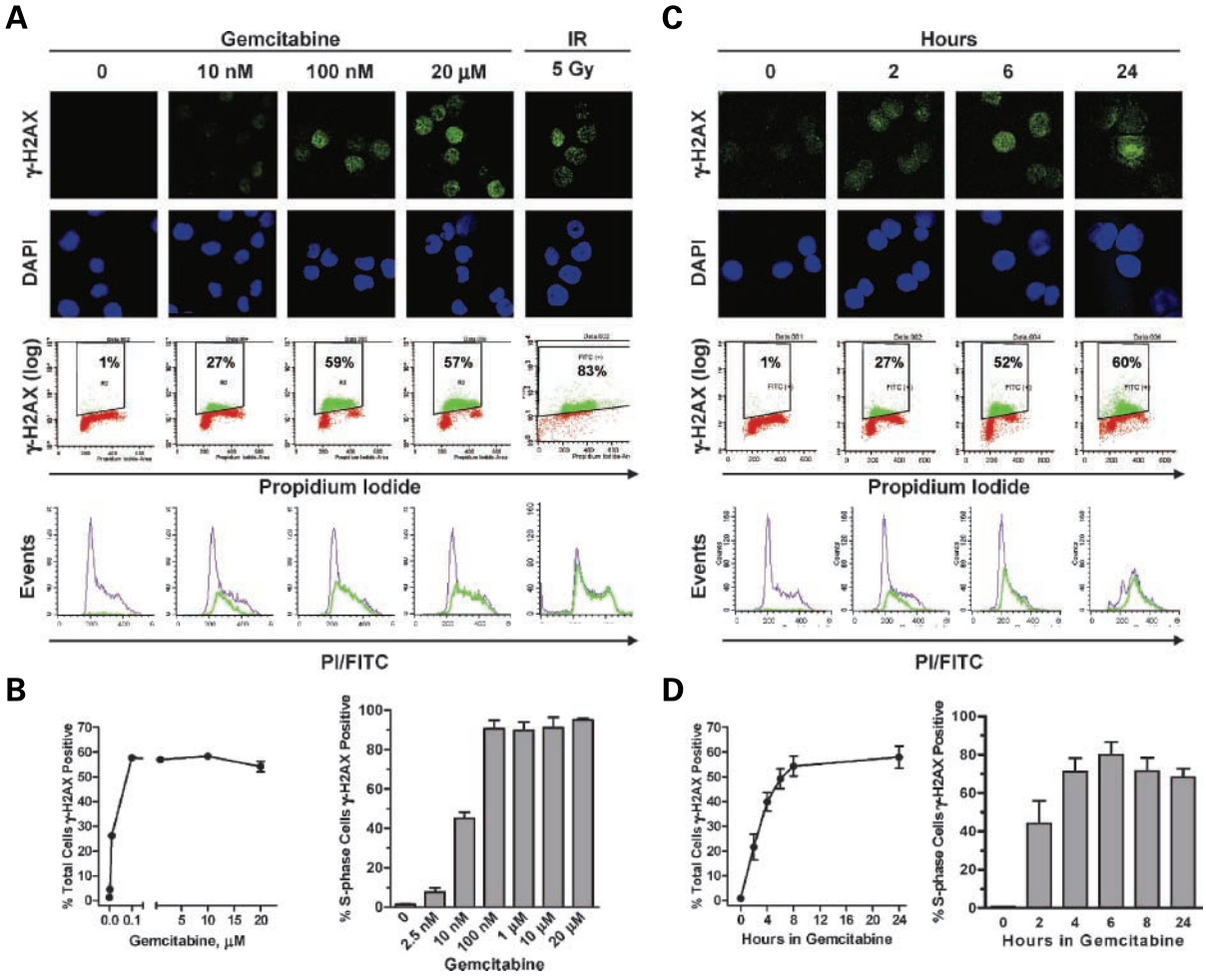

Figure 2. H2AX phosphorylation caused by gemcitabine-induced stalled replication forks. Exponentially growing cultures were incubated with 2.5 nmol/L to 20 μmol/L gemcitabine for 2 to 24 h or with 5 Gy ionizing radiation, harvested, and subjected to fluorescent staining of γ-H2AX. **A,** *top,* representative confocal microscopic images of γ-H2AX foci (*green*) and 4′,6-diamidino-2-phenylindole (*DAPI*) nuclear staining (*blue*) after exposure to gemcitabine for 2 h or to 5 Gy ionizing radiation (*IR*). *Middle,* cytometric analysis of γ-H2AX and propidium iodide staining of DNA content. Percentages of γ-H2AX – positive cells are shown for one experiment. *Bottom,* comparison of the total DNA content of the population (*purple*) versus the γ-H2AX – positive fraction (*green*). **B,** percentage of total (*left*) and S-phase (*right*) cells γ-H2AX positive within 2 h, as measured by flow cytometry. *Columns,* mean of three independent experiments ($n = 3$); *bars,* SE. *PI,* propidium iodide. **C,** H2AX phosphorylation in cultures exposed to 10 nmol/L gemcitabine for 2 to 24 h (same analysis as in **A**). **D,** percentage of total (*left*) and S-phase (*right*) cells with detected γ-H2AX after exposure to 10 nmol/L gemcitabine for 2 to 24 h. *Columns,* mean of three independent experiments ($n = 3$); *bars,* SE.

gemcitabine or other deoxycytidine nucleoside analogues, cytarabine (2) and troxacitabine (ref. 37; Supplementary Fig. S1A).[1]

Analysis of γ-H2AX by flow cytometry confirmed that H2AX phosphorylation was an early response to gemcitabine treatment and was concentration dependent (Supplementary Fig. S1B). An increase above the basal level of γ-H2AX was detected in ~25% of cells after treatment with 10 nmol/L gemcitabine for 2 h and was most apparent in the S-phase population (Fig. 2A, *middle* and *bottom*). The cellular fraction at the G_1-S border showed increased H2AX phosphorylation in response to the lowest drug concentration (Fig. 2A, *bottom*). Additionally, 55% to 60% of the total population exposed to 100 nmol/L gemcitabine had detectable γ-H2AX within 2 h, yet concentrations as great as 20 μmol/L failed to further enhance the percentage of cells with H2AX phosphorylation (Fig. 2B, *left*). Flow cytometric analysis of γ-H2AX, concurrent with analysis of cellular DNA content, showed that increases in H2AX phosphorylation were detectable in 90% of S-phase cells within 2 h of exposure to 0.1 to 20 μmol/L gemcitabine (Fig. 2B, *right*).

To establish the time dependency of gemcitabine-induced H2AX phosphorylation, cultures were exposed to 10 nmol/L gemcitabine for 2 to 24 h and immunofluorescent

[1] Supplementary material for this article are available at Molecular Cancer Therapeutics Online (http://mct.aacrjournals.org/).

γ-H2AX was examined as previously described. The levels of H2AX phosphorylation and nuclear foci formation increased within 6 h after exposure to gemcitabine (Fig. 2C). However, proportions of the population that were γ-H2AX positive did not exceed 60% during extended treatments (Fig. 2D, *left*). This is similar to when cultures were exposed to greater concentrations of gemcitabine (20 μmol/L) for only 2 h. H2AX phosphorylation was first detected within 2 h in the fraction of cells at the G_1-S border (Fig. 2C, *bottom*). Further, 70% to 80% of the S-phase population indicated an increase in H2AX phosphorylation on exposure to 10 nmol/L gemcitabine within 4 h, which did not further increase with time (Fig. 2D, *right*). These results likely reflect the S-phase specificity of gemcitabine and drug incorporation into DNA. In contrast, identification of γ-H2AX in cultures exposed to ionizing radiation did not show cell cycle phase specificity (Fig. 2A, *middle* and *bottom*). H2AX phosphorylation was detected by flow cytometry in ~85% (5 Gy) and 95% (10 Gy) of the total population within 2 h of ionizing radiation treatment (Fig. 2A; data not shown). The coincident decrease of [^{3}H]thymidine incorporation with the increase of γ-H2AX in S-phase cells on gemcitabine exposure indicates that phosphorylated H2AX may mark gemcitabine-induced stalled replication forks.

ATM Is Phosphorylated and Regulates H2AX Phosphorylation in Response to Gemcitabine

Because H2AX phosphorylation is regulated predominately by ATM in response to ionizing radiation, we investigated if ATM plays a role in H2AX phosphorylation after nucleoside analogue treatment. Flow cytometric analysis provided evidence that ATM is phosphorylated on Ser^{1981} within 2 h in response to 100 nmol/L gemcitabine (Fig. 3A, *top*). Similar to H2AX phosphorylation, ATM phosphorylation was predominantly associated with the S-phase fraction when cultures were exposed to gemcitabine, whereas ionizing radiation treatment did not reveal cell cycle phase specificity (Fig. 3A). Phosphorylated ATM formed nuclear foci that colocalized with γ-H2AX foci within 2 h of gemcitabine exposure, thus providing further evidence of H2AX regulation by ATM (Fig. 3B). Colocalization of γ-H2AX and phosphorylated ATM foci was also evident in OCI-AML3 cultures exposed to cytarabine or troxacitabine (data not shown). Inhibition of ATM, ATR, and DNA-dependent protein kinase before gemcitabine incubation with wortmannin or caffeine (38, 39) caused a decrease in γ-H2AX phosphorylation within 6 h by 25% and 55%, respectively (Fig. 3C). When cultures were preincubated with inhibitors in combination, γ-H2AX was undetectable within 2 h and inhibited by 75% at 6 h (Fig. 3C). H2AX phosphorylation was not observed after treatment with wortmannin and caffeine, alone or in combination (Fig. 3C). These investigations show that ATM is phosphorylated on Ser^{1981}, forms nuclear foci at sites of gemcitabine-induced DNA damage, and, possibly along with other related kinases, plays a role in mediating H2AX phosphorylation.

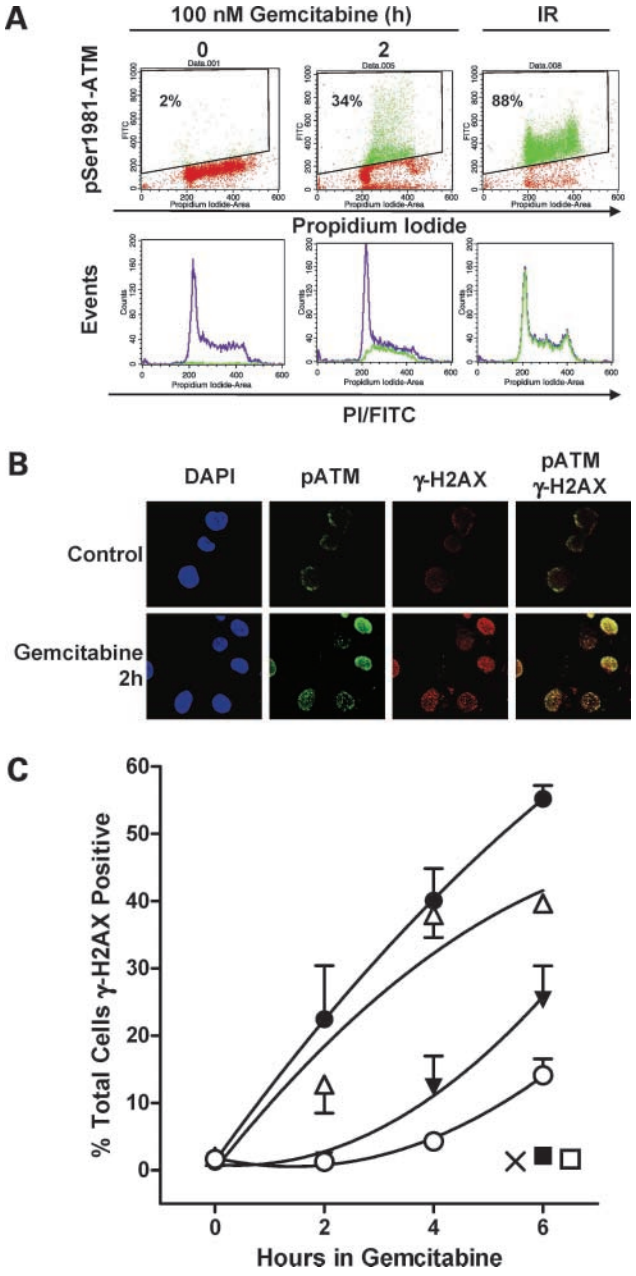

Figure 3. ATM is phosphorylated and regulates H2AX phosphorylation in response to gemcitabine-induced stalled replication forks. **A,** phosphorylation of Ser^{1981} on ATM versus DNA content (propidium iodide) after exposure to 100 nmol/L gemcitabine (2 h) or 10 Gy ionizing radiation (1 h). *Top,* percentages of phospho-ATM (Ser^{1981}) – positive cells (*pSer^{1981}-ATM*) for one experiment. *Bottom,* comparison of the total DNA content of the population (*purple*) versus the phospho-ATM (Ser^{1981}) – positive fraction (*green*). **B,** colocalization of phospho-ATM (Ser^{1981}) (*green*) and γ-H2AX (*red*) nuclear foci in response to gemcitabine (100 nmol/L, 2 h). **C,** cultures incubated with 10 nmol/L gemcitabine alone (●) or after preincubation with 10 μmol/L wortmannin (△) for 1 h, 5 mmol/L caffeine (▼) for 2 h, or both inhibitors in combination (○). Percentage of cells with increases in γ-H2AX was determined by flow cytometry. Neither treatment with wortmannin (■), caffeine (×), nor both inhibitors together (□) induced H2AX phosphorylation within 6 h when used in the absence of gemcitabine. *Points,* mean of three independent experiments (n = 3); *bars,* SE.

H2AX Phosphorylation Is Associated with the S-Phase Checkpoint

H2AX was phosphorylated in 60% of cells after exposure to gemcitabine (Fig. 2). This is likely the same fraction that arrests in S phase in response to gemcitabine-induced stalled replication forks (Fig. 1; ref. 5). It is possible that phosphorylation of H2AX is an indication of the early DNA damage sensor response that culminates in the activation of Chk1 and S-phase arrest. We investigated if γ-H2AX is associated with the S-phase checkpoint by analyzing the phosphorylation of checkpoint kinases that control cell cycle regulation. Phosphorylated forms of Chk1 (Ser^{317}) and Chk2 (Thr^{68}) were detected 24 to 33 h after exposure to gemcitabine (Fig. 4A). However, quantification of immunoblots did not reveal a significant increase in phosphorylation of Ser^{345} on Chk1. Consistent with an action of the S-phase checkpoint, the inactive Tyr^{15}-phosphorylated form of Cdk2 was identified by immunoblotting 24 to 33 h after gemcitabine treatment (Fig. 4A).

To measure increased DNA damage, we sought to enhance cytotoxicity by abrogating the S-phase checkpoint with the addition of a Chk1 inhibitor (UCN-01, 100 nmol/L).

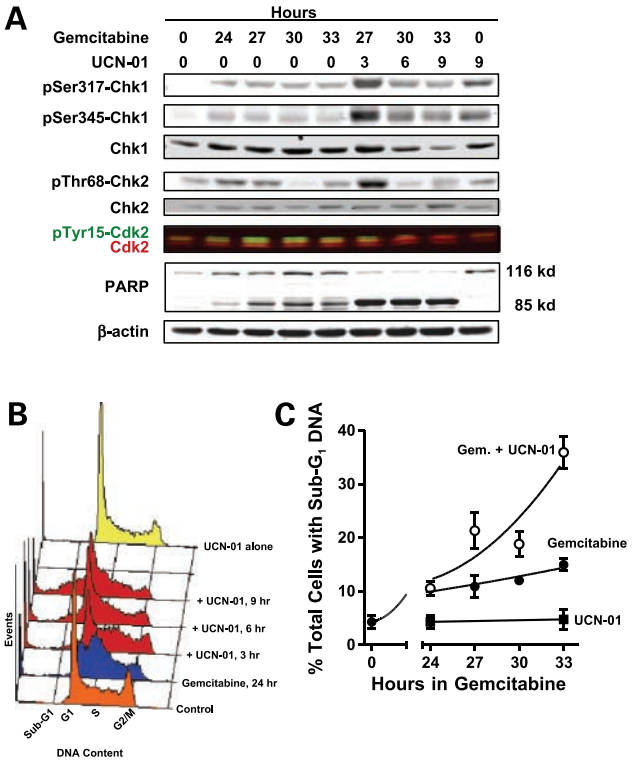

Figure 4. Effect of Chk1 inhibition on cultures previously exposed to gemcitabine. Exponentially growing cells were incubated with 10 nmol/L gemcitabine for 24 h before cultures were split and 100 nmol/L UCN-01 was added to one portion for 9 h. **A,** cell lysates were collected at indicated times and analyzed by immunoblotting with the appropriate antibodies. **B,** DNA content (propidium iodide) after exposure to gemcitabine, gemcitabine + UCN-01, or UCN-01 alone. **C,** percentage of cells with a sub-G_1 DNA content (propidium iodide) after exposure to gemcitabine (●), UCN-01 (■), or gemcitabine + UCN-01 (○). *Points,* mean of three independent experiments (n = 3); *bars,* SE.

Chk1 inhibition of S-phase arrested cultures resulted in a decrease in the number of S-phase cells (data not shown) and a substantial increase in cell death, as determined by sub-G_1 DNA content (Fig. 4B). Cell death was evident within 3 h and exceeded 35% 9 h after Chk1 inhibition (Fig. 4C). Single treatment with UCN-01 did not significantly affect the cell cycle or induce apoptosis (Fig. 4B and C). Apoptosis was associated with a further increase in phosphorylation of Chk1 (Ser^{317} and Ser^{345}) and Chk2 (Thr^{68}; Fig. 4A). Treatment with 100 nmol/L UCN-01 alone for 9 h also resulted in an increase in Chk1 phosphorylation (Fig. 4A; ref. 40). Dephosphorylation of Tyr^{15} on Cdk2 confirmed checkpoint abrogation and inhibition of Chk1 kinase (Fig. 4A). Ubiquitin-dependent degradation may be a cause for a decrease in total Chk1 protein 6 to 9 h after checkpoint dysregulation (41). Cleavage of poly(ADP-ribose) polymerase confirmed increases in apoptosis (Fig. 4A). Interestingly, gemcitabine treatment alone also induced cleavage of poly(ADP-ribose) polymerase to a lesser extent after treatment for >24 h, which may indicate that a fraction of cells are in the early stages of apoptosis. These experiments show that inhibition of Chk1 in S-phase–arrested cells induced further phosphorylation of Chk1 and Chk2, dephosphorylation of Cdk2, and cleavage of poly(ADP-ribose) polymerase.

Increased H2AX Phosphorylation Is Associated with Decreased Viability after Checkpoint Abrogation

Immunofluorescent γ-H2AX after Chk1 inhibition in gemcitabine-exposed cultures (10 nmol/L, 24 h) was investigated to determine if there was a difference in the extent of DNA damage after checkpoint abrogation. An intense increase in H2AX phosphorylation was evident on Chk1 inhibition (100 nmol/L UCN-01) within 3 h and was sustained for 9 h (Fig. 5A, *top*). Consistent with sub-G_1 DNA content and poly(ADP-ribose) polymerase cleavage, apoptotic cell morphology was evident after checkpoint abrogation within 3 h and was associated with cells intensely immunostained for γ-H2AX (Fig. 5A, *top*). When cultures were exposed to 10 nmol/L gemcitabine for only 2 h, γ-H2AX foci were evident, suggesting structural changes in the DNA or frank DNA damage, a precursor to checkpoint activation. Subsequent inhibition of Chk1 induced an intense increase in phosphorylation within 3 h (Fig. 5A, *middle*), resembling results after longer gemcitabine exposure times. A 10-fold increase in average γ-H2AX intensity was measured after Chk1 inhibition by flow cytometry on a comparison with gemcitabine alone–induced H2AX phosphorylation (Fig. 5B). Interestingly, the percentage of cells with detectable γ-H2AX (60%) did not increase as total phosphorylation levels intensified (Fig. 5C). This suggests that only the fraction of the population with gemcitabine-induced stalled replication forks shows dramatic increases in γ-H2AX upon checkpoint inhibition. To determine if the dramatic increases in H2AX phosphorylation were due to apoptosis-induced DNA fragmentation, cultures were pretreated with the pan-caspase inhibitor Z-VAD for 2 h before gemcitabine and UCN-01 exposure. Caspase inhibition blocked

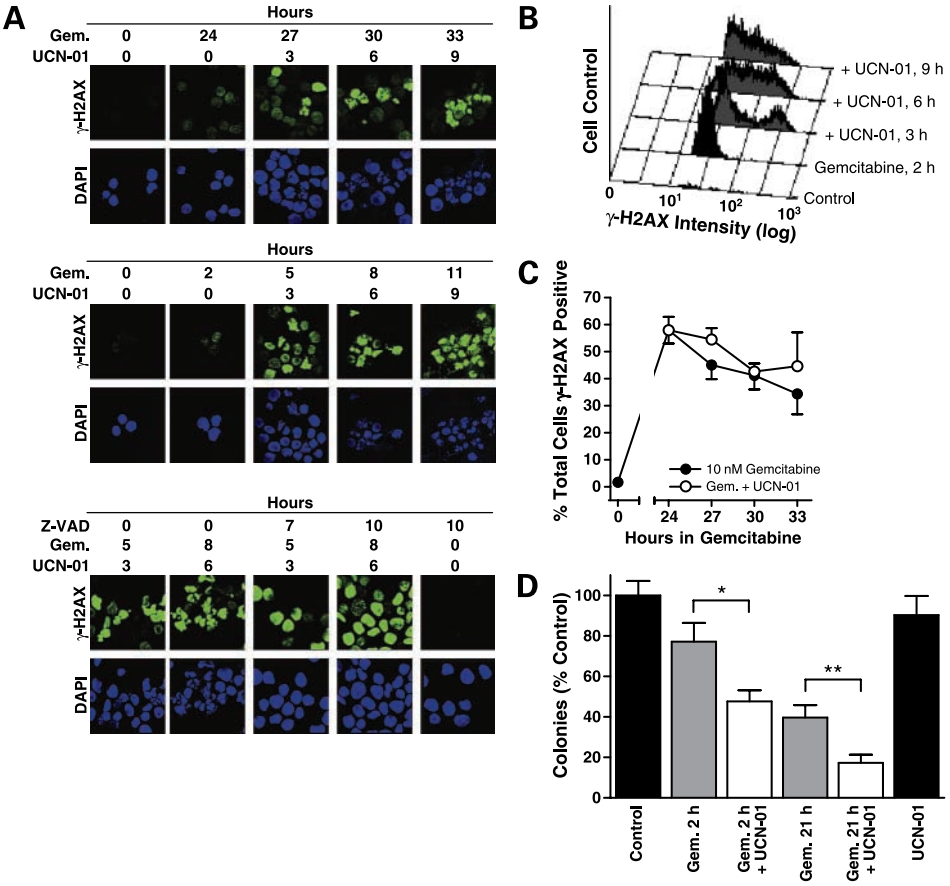

Figure 5. Effect of checkpoint abrogation on H2AX phosphorylation and cellular reproductive viability. Cells were incubated with combinations of 50 μmol/L Z-VAD, 10 nmol/L gemcitabine, and 100 nmol/L UCN-01 before cultures were harvested. **A,** representative images taken of immunostained γ-H2AX (*green*) and 4′,6-diamidino-2-phenylindole (DAPI) nuclear staining (*blue*) after exposure to combinations of Z-VAD, gemcitabine, and UCN-01. **B,** cytometric quantitation of H2AX phosphorylation after exposure to gemcitabine for 2 h ± UCN-01 for 3 to 9 h. **C,** percentage of cells that were γ-H2AX positive after treatment with gemcitabine (●) or gemcitabine + UCN-01 (○), determined by flow cytometry. *Points,* mean of three independent experiments ($n = 3$); *bars,* SE. **D,** percentage of cells that formed colonies (≥50 cells) within 10 d after 10 nmol/L gemcitabine, 100 nmol/L UCN-01, or gemcitabine + UCN-01. *Columns,* mean of three independent experiments ($n = 7-9$); *bars,* SE; *, $P < 0.001$; **, $P = 0.006$.

apoptosis-associated nuclear blebbing but did not inhibit increases in H2AX phosphorylation after checkpoint abrogation (Fig. 5A, *bottom*). These results confirm that increases in γ-H2AX after checkpoint abrogation are not due to apoptotic DNA fragmentation.

Clonogenic assays were done to determine if the clear increase in H2AX phosphorylation was associated with a decrease in cellular reproductive viability. Gemcitabine (10 nmol/L, 21 h) alone killed 65% of cells as compared with untreated cultures (Fig. 5D). In contrast, a significant decrease in viability (>80%) occurred when Chk1 was inhibited in S-phase–arrested cultures for 6 h before cell plating (Fig. 5D). Chk1 inhibition alone did not significantly affect viability. A considerable decrease in reproductive viability also occurred after Chk1 inhibition in cultures previously exposed to gemcitabine for only 2 h (Fig. 5D), thus showing the value of an intact S-phase checkpoint for overcoming stalled replication forks. These experiments establish that nuclear foci formation of γ-H2AX is associated with gemcitabine-induced stalled replication forks, whereas a pronounced increase in H2AX phosphorylation is associated with apoptosis.

Discussion

This study shows that H2AX is phosphorylated and forms distinct nuclear foci in response to nucleoside analogue–induced stalled replication forks. γ-H2AX increases were most apparent in the S-phase fraction, which is likely due to the S-phase specificity of these drugs (Fig. 2). In particular, cells at the G_1-S border were the first fraction of the total population to be measured as γ-H2AX positive. This possibly reflects that gemcitabine incorporation into DNA most rapidly occurs in cells initiating DNA synthesis. The same S-phase fraction of cells also showed phosphorylation of ATM on Ser^{1981}, a known regulator of H2AX and other DNA damage sensors (Fig. 3A). Ongoing investigations indicate that γ-H2AX colocalizes with DNA damage repair proteins shortly after nucleoside analogue exposure.[2] Inhibition of ATM and related kinases (ATR and DNA-dependent protein kinase) blocked H2AX phosphorylation (Fig. 3C), thus suggesting that this family of kinases participates in regulating H2AX phosphorylation after gemcitabine exposure.

Although the details of mammalian replication fork stabilization are poorly understood, the molecules associated with the S-phase checkpoint likely participate in

[2] B. Ewald, D. Sampath, and W. Plunkett. Colocalization of the Mre11-Rad50-Nbs1 complex, phosphorylated ATM, and γ-H2AX may identify sites of nucleoside analogue-induced stalled replication forks. AACR Meeting Abstracts 2007, Abstract #4037, unpublished.

maintaining fork structure (7). Downstream of Chk1 kinase, inhibition of Cdk2 leads to a decrease in replication origin firing, further protecting DNA replication fidelity (11). Our studies show that H2AX phosphorylation was associated with S-phase checkpoint activation in response to gemcitabine. It is unknown if H2AX participates in stabilization of stalled replication forks but it would be an explanation for rapid phosphorylation and nuclear foci formation. Activation of Chk1 kinase induced an accumulation of the inactive phosphorylated form of Cdk2, prompting S-phase arrest and suggesting inhibition of replication origin firing. Abrogation of the S-phase checkpoint by pharmacologic inhibition of Chk1 led to a significant increase in DNA damage, as marked by H2AX phosphorylation (Fig. 5). Interestingly, Chk1 inhibition caused an increase in H2AX phosphorylation and a decrease in reproductive viability when cultures were previously exposed to gemcitabine for only 2 h. This suggests that the S-phase checkpoint may be activated in response to gemcitabine-induced DNA damage as early as 2 h. The increased DNA damage after checkpoint abrogation is not due to apoptotic DNA fragmentation (Fig. 5A, *bottom*) and is likely caused by irreversible replication fork collapse, thus explaining a decrease in reproductive viability (Fig. 5D). An earlier study also showed increased H2AX phosphorylation after exposure to UCN-01 of cells previously treated with the topoisomerase I inhibitor camptothecin (42). Together, these results confirm the importance of an intact S-phase checkpoint for replication fork stabilization and cellular recovery from DNA-targeted therapeutics.

Although UCN-01 is known to have inhibitory activity against a number of kinases, the biological context of the present investigations implicates Chk1 as its target kinase. For instance, the IC_{50} of Chk1 (5–30 nmol/L; refs. 43, 44) is one of the lowest inhibitory values that have been reported. Two other kinases with low IC_{50}s include protein kinase C (5 nmol/L; ref. 45) and phosphoinositide-dependent kinase 1 (33 nmol/L; ref. 46). However, when used alone, UCN-01 did not affect phosphorylation of Akt, a target of phosphoinositide-dependent kinase 1, in exponentially growing ML-1 cells (15), nor was H2AX phosphorylation induced (data not shown; ref. 42). In addition, inhibition of protein kinase C by the specific inhibitor bisindolylmaleimide (GFX) did not abrogate the gemcitabine-induced S-phase checkpoint (data not shown). Other potential UCN-01 targets that are involved in the cell cycle have significantly higher IC_{50}s than concentrations used in this study, including Cdk1 (1 μmol/L; ref. 47), Cdk2 (>500 nmol/L; ref. 48), and Chk2 (1 μmol/L; ref. 43). Thus, the evidence indicates that the increased H2AX phosphorylation during checkpoint abrogation after exposure to UCN-01 is due to the inhibition of Chk1.

Nucleoside analogue exposure caused the formation of γ-H2AX nuclear foci at sites of stalled replication forks that resembled those that accumulate in response to ionizing radiation. Recently, Marti et al. (35) have reported that UV-C irradiation induces H2AX phosphorylation, which is seen as a diffuse, even, and pan-nuclear staining, but is not associated with double-strand breaks or apoptosis. They suggested that H2AX phosphorylation in response to UV-C may be associated with the excision of 6-4 photoproducts. We found that a similar, distinct γ-H2AX pan-nuclear staining occurs during checkpoint abrogation, but did not occur due to stalled DNA replication (Fig. 5A). In contrast to UV studies, the dramatic γ-H2AX increases measured here were associated with a decrease in clonogenic survival but were not caused by apoptosis-induced DNA fragmentation. This links elevated H2AX phosphorylation with a decreased capacity for cellular reproduction after checkpoint abrogation. Other reports have made similar correlations with γ-H2AX and apoptosis (27, 49). Therefore, intense pan-nuclear staining of γ-H2AX may signal that either DNA breaks are prevalent throughout the nucleus or DNA structure has been significantly compromised. However, it may only insinuate lethality under certain conditions. The phosphorylation increases in this study were likely due to irreparable collapsed replication forks that were the cause for decreased clonogenic survival. Interestingly, the fraction of cells with measurable H2AX phosphorylation did not increase upon checkpoint abrogation (Fig. 5C), suggesting that Chk1 inhibition specifically kills cells with an activated S-phase checkpoint. This occurred after only a 2-h exposure to gemcitabine, indicating that such pharmacologic interaction with checkpoint function can generate lethal damage.

H2AX phosphorylation after gemcitabine exposure was examined in this study. Other deoxycytidine nucleoside analogues with slightly different mechanisms of action, 1-β-D-arabinofuranosylcytosine and troxacitabine, induced similar levels of H2AX phosphorylation. Recent reports have shown that H2AX is phosphorylated on DNA polymerase and ribonucleotide reductase inhibition by aphidicolin and hydroxyurea, respectively (33, 50). Together, those investigations and this study suggest that H2AX is phosphorylated in response to agents that inhibit DNA synthesis. Thus, γ-H2AX may be useful for detection of pharmacodynamics of these drugs in the clinic. Measurement of H2AX phosphorylation by flow cytometry offers a novel technique for assessing nucleoside analogue DNA incorporation in primary samples in which there is a low incidence of cells in S phase (15). It may also offer insight into whether the drugs reach the tumor, are activated to their functional forms, and efficiently affect DNA synthesis.

The present results showed that 20 μmol/L gemcitabine exposure failed to increase H2AX phosphorylation above those achieved upon treatment with 100 nmol/L drug (Fig. 2). In addition, log-order apoptosis-associated increases in γ-H2AX occurred on checkpoint dysregulation in cultures treated with gemcitabine for only 2 h (Fig. 5), suggesting that prolonged exposure to nucleoside analogues is unnecessary to kill the S-phase fraction by this combinational strategy. Together, these results indicate that low-dose intermittent nucleoside analogue administration may be sufficient for S-phase checkpoint activation

and suggest a rationale for combinations with agents that dysregulate such defense mechanisms. Future studies aimed at a better understanding of the molecular mechanisms involved in recognizing nucleoside analogue–induced DNA damage may lead to identification of novel molecular targets that cause nucleoside analogue drug resistance.

References

1. Sampath D, Rao VA, Plunkett W. Mechanisms of apoptosis induction by nucleoside analogs. Oncogene 2003;22:9063 – 74.

2. Kufe DW, Major PP, Egan EM, Beardsley GP. Correlation of cytotoxicity with incorporation of ara-C into DNA. J Biol Chem 1980;255:8997 – 900.

3. Huang P, Chubb S, Hertel LW, Grindey GB, Plunkett W. Action of 2′,2′-difluorodeoxycytidine on DNA synthesis. Cancer Res 1991;51:6110 – 7.

4. Zhang YW, Hunter T, Abraham RT. Turning the replication checkpoint on and off. Cell Cycle 2006;5:125 – 8.

5. Shi Z, Azuma A, Sampath D, Li YX, Huang P, Plunkett W. S-Phase arrest by nucleoside analogues and abrogation of survival without cell cycle progression by 7-hydroxystaurosporine. Cancer Res 2001;61:1065 – 72.

6. Sampath D, Shi Z, Plunkett W. Inhibition of cyclin-dependent kinase 2 by the Chk1-25A pathway during the S-phase checkpoint activated by fludarabine: dysregulation by 7-hydroxystaurosporine. Mol Pharmacol 2002;62:680 – 8.

7. Lopes M, Cotta-Ramusino C, Pellicioli A, et al. The DNA replication checkpoint response stabilizes stalled replication forks. Nature 2001;412:557 – 61.

8. Huang P, Chubb S, Plunkett W. Termination of DNA synthesis by 9-β-D-arabinofuranosyl-2-fluoroadenine. A mechanism for cytotoxicity. J Biol Chem 1990;265:16617 – 25.

9. Chen Y, Sanchez Y. Chk1 in the DNA damage response: conserved roles from yeasts to mammals. DNA Repair (Amst) 2004;3:1025 – 32.

10. Busino L, Chiesa M, Draetta GF, Donzelli M. Cdc25A phosphatase: combinatorial phosphorylation, ubiquitylation and proteolysis. Oncogene 2004;23:2050 – 6.

11. Mailand N, Diffley JF. CDKs promote DNA replication origin licensing in human cells by protecting Cdc6 from APC/C-dependent proteolysis. Cell 2005;122:915 – 26.

12. Kohn EA, Ruth ND, Brown MK, Livingstone M, Eastman A. Abrogation of the S phase DNA damage checkpoint results in S phase progression or premature mitosis depending on the concentration of 7-hydroxystaurosporine and the kinetics of Cdc25C activation. J Biol Chem 2002;277:26553 – 64.

13. Arlander SJ, Eapen AK, Vroman BT, McDonald RJ, Toft DO, Karnitz LM. Hsp90 inhibition depletes Chk1 and sensitizes tumor cells to replication stress. J Biol Chem 2003;278:52572 – 7.

14. Shao RG, Cao CX, Pommier Y. Abrogation of Chk1-mediated S/G_2 checkpoint by UCN-01 enhances ara-C-induced cytotoxicity in human colon cancer cells. Acta Pharmacol Sin 2004;25:756 – 62.

15. Sampath D, Cortes J, Estrov Z, et al. Pharmacodynamics of cytarabine alone and in combination with 7-hydroxystaurosporine (UCN-01) in AML blasts *in vitro* and during a clinical trial. Blood 2006;107:2517 – 24.

16. Kortmansky J, Shah MA, Kaubisch A, et al. Phase I trial of the cyclin-dependent kinase inhibitor and protein kinase C inhibitor 7-hydroxystaurosporine in combination with Fluorouracil in patients with advanced solid tumors. J Clin Oncol 2005;23:1875 – 84.

17. Lara PN, Jr., Mack PC, Synold T, et al. The cyclin-dependent kinase inhibitor UCN-01 plus cisplatin in advanced solid tumors: a California cancer consortium phase I pharmacokinetic and molecular correlative trial. Clin Cancer Res 2005;11:4444 – 50.

18. Zhou B-BS, Elledge SJ. The DNA damage response: putting checkpoints in perspective. Nature 2000;408:433 – 9.

19. Bakkenist CJ, Kastan MB. DNA damage activates ATM through intermolecular autophosphorylation and dimer dissociation. Nature 2003;421:499 – 506.

20. Bekker-Jensen S, Lukas C, Kitagawa R, et al. Spatial organization of the mammalian genome surveillance machinery in response to DNA strand breaks. J Cell Biol 2006;173:195 – 206.

21. Burma S, Chen BP, Murphy M, Kurimasa A, Chen DJ. ATM phosphorylates histone H2AX in response to DNA double-strand breaks. J Biol Chem 2001;276:42462 – 7.

22. Fernandez-Capetillo O, Lee A, Nussenzweig M, Nussenzweig A. H2AX: the histone guardian of the genome. DNA Repair (Amst) 2004;3:959 – 67.

23. Rogakou EP, Boon C, Redon C, Bonner WM. Megabase chromatin domains involved in DNA double-strand breaks *in vivo*. J Cell Biol 1999;146:905 – 16.

24. Rogakou EP, Pilch DR, Orr AH, Ivanova VS, Bonner WM. DNA double-stranded breaks induce histone H2AX phosphorylation on serine 139. J Biol Chem 1998;273:5858 – 68.

25. Downey M, Durocher D. γH2AX as a checkpoint maintenance signal. Cell Cycle 2006;5:1376 – 81.

26. Xie A, Puget N, Shim I, et al. Control of sister chromatid recombination by histone H2AX. Mol Cell 2004;16:1017 – 25.

27. Mukherjee B, Kessinger C, Kobayashi J, et al. DNA-PK phosphorylates histone H2AX during apoptotic DNA fragmentation in mammalian cells. DNA Repair (Amst) 2006;5:575 – 90.

28. Lu C, Zhu F, Cho YY, et al. Cell apoptosis: requirement of H2AX in DNA ladder formation, but not for the activation of caspase-3. Mol Cell 2006;23:121 – 32.

29. Chowdhury D, Keogh MC, Ishii H, Peterson CL, Buratowski S, Lieberman J. γ-H2AX dephosphorylation by protein phosphatase 2A facilitates DNA double-strand break repair. Mol Cell 2005;20:801 – 9.

30. Bassing CH, Suh H, Ferguson DO, et al. Histone H2AX: a dosage-dependent suppressor of oncogenic translocations and tumors. Cell 2003;114:359 – 70.

31. Celeste A, Petersen S, Romanienko PJ, et al. Genomic instability in mice lacking histone H2AX. Science 2002;296:922 – 7.

32. Bassing CH, Chua KF, Sekiguchi J, et al. Increased ionizing radiation sensitivity and genomic instability in the absence of histone H2AX. Proc Natl Acad Sci U S A 2002;99:8173 – 8.

33. Ward IM, Chen J. Histone H2AX is phosphorylated in an ATR-dependent manner in response to replicational stress. J Biol Chem 2001;276:47759 – 62.

34. Olive PL, Banath JP, Sinnott LT. Phosphorylated histone H2AX in spheroids, tumors, and tissues of mice exposed to etoposide and 3-amino-1,2,4-benzotriazine-1,3-dioxide. Cancer Res 2004;64:5363 – 9.

35. Marti TM, Hefner E, Feeney L, Natale V, Cleaver JE. H2AX phosphorylation within the G_1 phase after UV irradiation depends on nucleotide excision repair and not DNA double-strand breaks. Proc Natl Acad Sci U S A 2006;103:9891 – 6.

36. Karnitz LM, Flatten KS, Wagner JM, et al. Gemcitabine-induced activation of checkpoint signaling pathways that affect tumor cell survival. Mol Pharmacol 2005;68:1636 – 44.

37. Grove KL, Cheng YC. Uptake and metabolism of the new anticancer compound β-L-(−)-dioxolane-cytidine in human prostate carcinoma DU-145 cells. Cancer Res 1996;56:4187 – 91.

38. Sarkaria J, Tibbetts R, Busby E, Kennedy A, Hill D, Abraham R. Inhibition of phosphoinositide 3-kinase related kinases by the radiosensitizing agent wortmannin. Cancer Res 1998;58:4375 – 82.

39. Sarkaria JN, Busby EC, Tibbetts RS, et al. Inhibition of ATM and ATR kinase activities by the radiosensitizing agent, caffeine. Cancer Res 1999;59:4375 – 82.

40. Syljuasen RG, Sorensen CS, Hansen LT, et al. Inhibition of human Chk1 causes increased initiation of DNA replication, phosphorylation of ATR targets, and DNA breakage. Mol Cell Biol 2005;25:3553 – 62.

41. Zhang YW, Otterness DM, Chiang GG, et al. Genotoxic stress targets human Chk1 for degradation by the ubiquitin-proteasome pathway. Mol Cell 2005;19:607 – 18.

42. Furuta T, Hayward RL, Meng LH, et al. p21CDKN1A allows the repair of replication-mediated DNA double-strand breaks induced by topoisomerase I and is inactivated by the checkpoint kinase inhibitor 7-hydroxystaurosporine. Oncogene 2006;25:2839 – 49.

43. Busby EC, Leistritz DF, Abraham RT, Karnitz LM, Sarkaria JN. The radiosensitizing agent 7-hydroxystaurosporine (UCN-01) inhibits the DNA damage checkpoint kinase hChk1. Cancer Res 2000;60:2108 – 12.

44. Jackson JR, Gilmartin A, Imburgia C, Winkler JD, Marshall LA, Roshak A. An indolocarbazole inhibitor of human checkpoint kinase (Chk1) abrogates cell cycle arrest caused by DNA damage. Cancer Res 2000;60:566 – 72.

45. Takahashi I, Saitoh Y, Yoshida M, et al. UCN-01 and UCN-02, new

selective inhibitors of protein kinase C. II. Purification, physico-chemical properties, structural determination and biological activities. J Antibiot (Tokyo) 1989;42:571 – 6.

46. Sato S, Fujita N, Tsuruo T. Interference with PDK1-Akt survival signaling pathway by UCN-01 (7-hydroxystaurosporine). Oncogene 2002; 21:1727 – 38.

47. Wang Q, Worland PJ, Clark JL, Carlson BA, Sausville EA. Apoptosis in 7-hydroxystaurosporine-treated T lymphoblasts correlates with activation of cyclin-dependent kinases 1 and 2. Cell Growth Differ 1995;6: 927 – 36.

48. Akiyama T, Yoshida T, Tsujita T, et al. G_1 phase accumulation induced by UCN-01 is associated with dephosphorylation of Rb and CDK2 proteins as well as induction of CDK inhibitor p21/Cip1/WAF1/Sdi1 in p53-mutated human epidermoid carcinoma A431 cells. Cancer Res 1997; 57:1495 – 501.

49. Huang X, Halicka HD, Traganos F, Tanaka T, Kurose A, Darzynkiewicz Z. Cytometric assessment of DNA damage in relation to cell cycle phase and apoptosis. Cell Prolif 2005;38:223 – 43.

50. Kurose A, Tanaka T, Huang X, Traganos F, Dai W, Darzynkiewicz Z. Effects of hydroxyurea and aphidicolin on phosphorylation of ataxia telangiectasia mutated on Ser 1981 and histone H2AX on Ser 139 in relation to cell cycle phase and induction of apoptosis. Cytometry A 2006;69:212 – 21.